

RESEARCH ARTICLE

# ALC1/CHD1L, a chromatin-remodeling enzyme, is required for efficient base excision repair

Masataka Tsuda<sup>1</sup>✉, Kosai Cho<sup>1,2</sup>✉, Masato Ooka<sup>3</sup>, Naoto Shimizu<sup>1</sup>, Reiko Watanabe<sup>4</sup>✉, Akira Yasui<sup>4</sup>, Yuka Nakazawa<sup>5,6</sup>, Tomoo Ogi<sup>5,6</sup>, Hiroshi Harada<sup>7</sup>, Keli Agama<sup>8</sup>, Jun Nakamura<sup>9</sup>, Ryuta Asada<sup>3</sup>, Haruna Fujii<sup>1</sup>, Tetsushi Sakuma<sup>10</sup>, Takashi Yamamoto<sup>10</sup>, Junko Murai<sup>1,8</sup>, Masahiro Hiraoka<sup>11</sup>, Kaoru Koike<sup>2</sup>, Yves Pommier<sup>8</sup>, Shunichi Takeda<sup>1\*</sup>, Kouji Hirota<sup>1,3\*</sup>



**1** Department of Radiation Genetics, Graduate School of Medicine, Kyoto University, Yoshidakonoe, Sakyo-ku, Kyoto, Japan, **2** Department of Primary Care and Emergency Medicine, Kyoto University Graduate School of Medicine, Sakyo-ku, Kyoto, Japan, **3** Department of Chemistry, Tokyo Metropolitan University, Minami-Osawa, Hachioji-shi, Tokyo, Japan, **4** Division of Dynamic Proteome, Institute of Development, Aging and Cancer, Tohoku University, Seiryomachi 4-1, Aobaku, Sendai, Japan, **5** Department of Genome Repair, Atomic Bomb Disease Institute, Nagasaki University Sakamoto, Nagasaki, Japan, **6** Department of Genetics, Research Institute of Environmental Medicine (RIEM), Nagoya University, Furo-cho, Chikusa-ku, Nagoya, Japan, **7** Laboratory of Cancer Cell Biology, Radiation Biology Center, Kyoto University, Yoshidakonoe, Sakyo-ku, Kyoto, Japan, **8** Laboratory of Molecular Pharmacology, Developmental Therapeutics Branch, Center for Cancer Research, National Cancer Institute, National Institutes of Health, Bethesda, MD, United States of America, **9** Department of Environmental Sciences and Engineering, University of North Carolina Chapel Hill, North Carolina, United States of America, **10** Department of Mathematical and Life Sciences, Graduate School of Science, Hiroshima University, Hiroshima, Japan, **11** Department of Radiation Oncology, Japanese Red Cross Society Wakayama Medical Center, Komatsubara-Dori, Wakayama, Japan

✉ These authors contributed equally to this work.

✉ Current address: National Institutes of Biomedical Innovation, Health and Nutrition, Osaka, Japan

\* [khirota@tmu.ac.jp](mailto:khirota@tmu.ac.jp) (KH); [stakeda@rg.med.kyoto-u.ac.jp](mailto:stakeda@rg.med.kyoto-u.ac.jp) (ST)

OPEN ACCESS

**Citation:** Tsuda M, Cho K, Ooka M, Shimizu N, Watanabe R, Yasui A, et al. (2017) ALC1/CHD1L, a chromatin-remodeling enzyme, is required for efficient base excision repair. PLoS ONE 12(11): e0188320. <https://doi.org/10.1371/journal.pone.0188320>

**Editor:** Robert W. Sobol, University of South Alabama Mitchell Cancer Institute, UNITED STATES

**Received:** July 19, 2017

**Accepted:** November 3, 2017

**Published:** November 17, 2017

**Copyright:** This is an open access article, free of all copyright, and may be freely reproduced, distributed, transmitted, modified, built upon, or otherwise used by anyone for any lawful purpose. The work is made available under the [Creative Commons CC0](https://creativecommons.org/licenses/by/4.0/) public domain dedication.

**Data Availability Statement:** All relevant data are within the paper and its Supporting Information files.

**Funding:** This work was supported by the JSPS KAKENHI Grant Number (JP16K12598, JP16H02957 and JP16H01314 to KH, JP16H06306 to ST and JP16J02252 to RA), the JSPS Core-to-Core Program (A) Advanced Research Networks (to ST), the Takeda Science Foundation and Yamada Science Foundation (to KH), and the Center for Cancer Research,

## Abstract

ALC1/CHD1L is a member of the SNF2 superfamily of ATPases carrying a macrodomain that binds poly(ADP-ribose). Poly(ADP-ribose) polymerase (PARP) 1 and 2 synthesize poly(ADP-ribose) at DNA-strand cleavage sites, promoting base excision repair (BER). Although depletion of ALC1 causes increased sensitivity to various DNA-damaging agents (H<sub>2</sub>O<sub>2</sub>, UV, and phleomycin), the role played by ALC1 in BER has not yet been established. To explore this role, as well as the role of ALC1's ATPase activity in BER, we disrupted the *ALC1* gene and inserted the ATPase-dead (E165Q) mutation into the *ALC1* gene in chicken DT40 cells, which do not express PARP2. The resulting *ALC1*<sup>-/-</sup> and *ALC1*<sup>-/E165Q</sup> cells displayed an indistinguishable hypersensitivity to methylmethane sulfonate (MMS), an alkylating agent, and to H<sub>2</sub>O<sub>2</sub>, indicating that ATPase plays an essential role in the DNA-damage response. *PARP1*<sup>-/-</sup> and *ALC1*<sup>-/-</sup>/*PARP1*<sup>-/-</sup> cells exhibited a very similar sensitivity to MMS, suggesting that ALC1 and PARP1 collaborate in BER. Following pulse-exposure to H<sub>2</sub>O<sub>2</sub>, *PARP1*<sup>-/-</sup> and *ALC1*<sup>-/-</sup>/*PARP1*<sup>-/-</sup> cells showed similarly delayed kinetics in the repair of single-strand breaks, which arise as BER intermediates. To ascertain ALC1's role in BER in mammalian cells, we disrupted the *ALC1* gene in human TK6 cells. Following exposure to MMS and to H<sub>2</sub>O<sub>2</sub>, the *ALC1*<sup>-/-</sup> TK6 cell line showed a delay in single-strand-break repair.

Intramural Program of the US National Cancer Institute (Z01 BC 006150 to KA and YP). The funders had no role in study design, data collection and analysis, decision to publish, or preparation of the manuscript.

**Competing interests:** The authors have declared that no competing interests exist.

We therefore conclude that ALC1 plays a role in BER. Following exposure to H<sub>2</sub>O<sub>2</sub>, *ALC1*<sup>-/-</sup> cells showed compromised chromatin relaxation. We thus propose that ALC1 is a unique BER factor that functions in a chromatin context, most likely as a chromatin-remodeling enzyme.

## Introduction

Base excision repair (BER) eliminates nucleotides damaged by oxidation, alkylation, and hydrolysis. There are complex variations within the BER process (for review, see references [1, 2]). A typical BER is initiated by enzymatic removal of the damaged base, leading to the formation of apurinic/aprimidinic (AP) sites, followed by incision of the DNA backbone at the AP sites, yielding single-strand breaks (SSBs). Since SSB repair and BER share a number of repair factors, such as Poly(ADP-ribose) polymerase (PARP) 1 and 2, SSB repair is considered a specialized BER sub-pathway [3]. PARP1 and PARP2 accumulate quickly at SSB sites, and PARylate themselves as well as chromatin proteins. Poly(ADP-ribose) (PAR) facilitates the recruitment of x-ray-repair cross-complementing group 1 (XRCC1) [4]. XRCC1 plays a key role in SSB repair by providing docking sites for critical effector molecules, polynucleotide kinase 3'-phosphatase (PNKP), DNA polymerase β (Polβ), and ligase 3. PNKP and Polβ restore hydroxyl and phosphorylation residues at the 3' and 5' ends, respectively, of the SSBs. Polβ incorporates a single nucleotide, a process called short-patch repair synthesis, for subsequent ligation of SSBs. Polβ, Polδ, and Polθ, on the other hand, undergo long-patch repair synthesis, involving 2–12 nucleotide incorporation, by strand-displacement synthesis, generating a 5' flap. The Fen-1 endonuclease removes the 5' flap for subsequent ligation.

Recent studies indicate that PAR is recognized by ALC1 (amplified in liver cancer 1, also known as CHD1L [chromodomain-helicase-DNA-binding protein 1-like]) at its carboxy terminal [5, 6]. ALC1 is a member of the SNF2 superfamily of ATPases, which can function as chromatin-remodeling enzymes [7–9]. ALC1 is believed to play multiple roles in various DNA-damage responses, since depletion of ALC1 causes hypersensitivity to UV, H<sub>2</sub>O<sub>2</sub>, and phleomycin [6, 10], which induce lesions repaired primarily by nucleotide excision repair, BER, and double-strand break (DSB) repair, respectively. The role played by PARP in both the SSB- and DSB-repair pathways, and the conversion of SSBs to DSBs during DNA replication, make the hypersensitivity of ALC1-depleted cells very difficult to interpret. Another complexity of ALC1's role is involvement of ALC1 in transcriptional control for effective DNA-damage responses, as evidenced by the observation that ALC1 interacts with Tripartite Motif-containing 33 (TRIM33), a multifunctional protein implicated in transcriptional regulation [11]. Collectively, whether or not ALC1 promotes BER has remained elusive, and the functional relationship between ALC1 and PARP1 has been also undefined.

We disrupted the *ALC1* gene in the human TK6 and chicken DT40 B cell lines. We also disrupted the *ALC1* gene in PARP1-deficient DT40 cells. DT40 has a unique advantage for reverse-genetic study of the PARP enzyme due to the absence of the *PARP2* gene in the chicken genome [12]. Note that the chicken *XRCC1* ortholog gene has not yet been identified. PARP1-deficient *PARP1*<sup>-/-</sup> DT40 cells show an increased methylmethane sulfonate (MMS) sensitivity and a marked accumulation of SSBs [13]. We found that *ALC1*<sup>-/-</sup>, *PARP1*<sup>-/-</sup>, and *ALC1*<sup>-/-</sup>/*PARP1*<sup>-/-</sup> DT40 cells were markedly sensitive to both H<sub>2</sub>O<sub>2</sub> and MMS, suggesting that ALC1 collaborates with PARP1-mediated BER. We examined the role played by ALC1 in BER by conducting alkaline-comet and alkaline-elusion assays, which are the established methods of monitoring ongoing BER [14, 15]. Our data demonstrate that ALC1 promotes BER in both

TK6 and DT40 cells. We conclude that ALC1 plays a critical role in BER, under the control of PARP1.

## Materials and methods

### DT40-cell culture, cell counting, and cell-cycle analysis

DT40 cell line was from Takeda laboratory (Kyoto University) [16]. Culture conditions for the chicken DT40 cells, cell counting, and cell-cycle analysis were as described previously [17–20].

### TK6-cell culture

TK6 cell line was purchased from JCRB cell bank (<http://cellbank.nibiohn.go.jp/english/>). TK6 cells [21] were cultured in an RPMI 1640 medium (Nacalai Tesque, Kyoto, Japan) supplemented with 10% heat-inactivated horse serum (HS) (GIBCO, lot No. 2017–06), 0.1 mM sodium pyruvate, L-glutamin (Nacalai Tesque), 50 U/mL penicillin, and 50 µg/mL streptomycin (Nacalai Tesque). TK6 has a stable, near-diploid karyotype, though it carries a trisomic chromosome 13 [22].

### si-RNA treatment

HeLa and U2OS cells were cultured in DMEM supplemented with 10% fetal-calf serum at 37° C. si-RNAs for the depletion of ALC1 and the control were purchased from Thermo Scientific (Dharmacon si-RNA, PA).  $3 \times 10^5$  cells were transfected with 250 pmol si-RNA using 10 µl Lipofectamine RNAiMAX (Invitrogen, CA).

### Genotoxic reagents

H<sub>2</sub>O<sub>2</sub> (Nacalai) and MMS (Nacalai) were used for the sensitivity assay, as described previously [23].

### Measurement of sensitivity to genotoxic agents in DT40 and TK6 cells

10<sup>6</sup> DT40 cells were exposed to H<sub>2</sub>O<sub>2</sub> and MMS for 1 h in 1 ml culture medium and PBS containing 1% fetal bovine serum, respectively. TK6 cells were exposed to the two DNA-damaging agents in the same manner. 0.01 ml cell suspensions (containing 10<sup>4</sup> cells) of the exposed DT40 or TK6 cells were plated in duplicate onto 24-well cluster plates containing 1 ml of the complete medium, and were incubated for 48 h (for DT40) and 72 h (for TK6). To measure the number of living cells, we transferred 100 µl cell suspensions to the individual wells of 96-well plates and measured the amount of ATP in the cellular lysates using CellTiter-Glo (Promega), according to the manufacturer's instructions. Luminescence was measured with Fluoroskan Ascent FL (Thermo Fisher Scientific Inc., Pittsburgh, PA).

### Generation of *ALC1* targeting constructs for DT40 cells

*ALC1* targeting constructs were generated from genomic PCR products combined with *BSR*<sup>R</sup> or *HIS*<sup>R</sup> selection-marker cassettes. Genomic DNA sequences were amplified using primers 5'–CCGGAATTCTTACACCCAGGCACACAAAA–3' and 5'–CGCGGATCCCTGGAAGCCAC CAGAAGAAG–3' (for the left arm), and 5'–CGCGGATCCCATGGCAGTGAAACATGGAC–3' and 5'–ATTGCGGCCCGCCTGCAATGCAAAAGACCTGA–3' (for the right arm). The resulting amplified fragments were inserted into the *EcoRI* and *NotI* sites of pBluescript II (Stratagene). Marker-gene cassettes, *BSR*<sup>R</sup> and *HIS*<sup>R</sup>, were then inserted into the *BamHI* site of the resulting plasmid to generate *ALC1-BER* and *ALC1-HIS* gene-targeting constructs. A probe for Southern

blot was amplified from DT40 genomic DNA using primers 5' -AAACGTTACGCCCTTAGGC TCGTTGCTTCTT-3' and 5' -CATCTGTGATTCTATGTTTTTCAGCTTC-3'.

### Generation of *ALC1*<sup>-/-</sup> and *ALC1*<sup>-/-</sup>/*PARP1*<sup>-/-</sup> mutant DT40 cells

We sequentially transfected *ALC1*-BSR- and then *ALC1*-HIS-targeting constructs to obtain *ALC1*<sup>-/-</sup> cells from *wild-type* DT40 cells. Similarly, we generated *ALC1*<sup>-/-</sup>/*PARP1*<sup>-/-</sup> mutant clones from *PARP1*<sup>-/-</sup> cells [24].

### Generation of *ALC1*<sup>-/E165Q</sup> mutant DT40 cells

To selectively inactivate the ATPase activity of ALC1, we generated an E165Q mutation knock-in construct carrying the *HIS*<sup>R</sup> selection-marker cassette. Genomic DNA sequences were amplified using primers 5' -TGAGCAACTGGAAGGAGGAGCTGGAGAG-3' and 5' -AA AAGTCTTTATACAGTACAAGATAGCTGG-3' (for the left arm), and 5' -GGGATCCCCTATA GGATACAGATTTTCTGTTTATTC-3' and 5' - TTCTAGAACTTACCTGGCTCACTCTCCTT TTCAACTG-3' (for the right arm). The amplified fragment for the left arm was mutated using primers 5' -GCCTTGTTGTAGATCAAGCTCACAGGCTG-3' and 5' -CAGCCTGTG AGCTTGATCTACAACCAAGGC-3' (the E to Q mutation is associated with the underlined *Sau*3AI site). The obtained left arm and the right arm were cloned into Zero Blunt TOPO (Invitrogen, CA). The 3.9 kb *XhoI*/*Bam*HI fragment from the left arm and the 1.4 kb *Bam*HI/*XbaI* fragment from the right arm were inserted into the *XhoI*/*XbaI* site of pBluescript vector (Stratagene). A marker-gene cassette, loxP-flanked *HIS*<sup>R</sup>, was then inserted into the *Bam*HI site of the resulting plasmid to generate the E165Q mutation knock-in construct. The *ALC1*<sup>-/+</sup> cells were then transfected with the E165Q mutation knock-in construct to obtain *ALC1*<sup>-/E165Q</sup> cells. Targeted integration into the *wild-type* allele was confirmed by Southern blot analysis of *Bam*HI-digested genomic DNA, with the use of an internal probe prepared from a 1.0 kb *Eco*RI fragment in the left arm using a Random Primer kit (GE Healthcare, UK). To delete the loxP-flanked *HIS*<sup>R</sup> cassette, a Cre expression vector was transiently transfected using *Amaxa*<sup>™</sup> Nucleofector<sup>™</sup> 2b (Lonza) and then incubated for 48 h in medium containing tamoxifen. We performed limiting dilution of cells and isolated clones. RT-PCR was then performed for individual clones, using primers 5' -CCTGATACTTTGTCTCTGTCTGTTCTGAG-3' and 5' -T CCAATCTCAAAGGGCTCCGGCTCAACACC-3'. The knock-in mutation was screened by identifying 0.24 kb + 0.49 kb *Sau*3AI-digested fragments in the amplified PCR product, and was verified by nucleotide sequencing.

### Generation of *ALC1*<sup>-/-</sup> mutant TK6 cells

*ALC1* targeting vector was constructed to replace part of the 8th exon with a resistance (*Puro* and *Neo*)-gene cassette flanked by loxP signals at both ends. The primers used to amplify the left arm were 5' -CCTCGAGCTCAGTAGTCTTCAGTCTCCTGTTGAC-3' and 5' -GGCTAGC GCTGCAAGAGTTTGTGCAGTTCACTTG-3', and the primers for the right arm were 5' -GGC GGCCGCGCATTCAGAAATACTACAAGGCC-3' and 5' -GGTCGACATATGGGTGATC CACACACTTTTCGAAG. Expression vector for transcription activator-like effector nuclease (TALEN) was designed to recognize the following sequences according to the method described in Sakuma *et al* [25]: 5' -TGCACAACTCTTGCAG-3' and 5' -CGAGTGAAAGCTGA GGTA-3'. To generate *ALC1*<sup>-/-</sup> cells, *wild-type* TK6 cells were transfected with the *ALC1* targeting vectors (*Puro*<sup>R</sup> and *Neo*<sup>R</sup>) with expression vector for TALEN using NEON transfection system (Invitrogen, CA) at 1500 V 20 msec. The loss of *ALC1* transcript was confirmed by RT-PCR using primers 5' - CAAGAAGACA GAAGTAGTGA TATACCATGG-3' and 5' - CCA TATAGTCTTGGAGAATATCCAACATCT-3'. *GAPDH* transcripts were analyzed as a positive

control for the RT-PCR analysis using primers 5' – TGGCCAAGGTCATCCATGACAACTT–3' and 5' – GCGCCAGTAGAGGCAGGGATGATGT –3'. The loss of ALC1 protein was confirmed by western blot using anti-ALC1 antibody (abcam, ab51324).  $\beta$ -actin was detected using specific antibody (Sigma, A5441) as a loading control.

### Determination of intracellular NAD(P)H concentration

The cellular NAD(P)H concentration was determined as previously described [26].

### Detection of GFP-XRCC1 at the site of SSBs induced by *Neurospora crassa* UV-damage endonuclease (UVDE)

Local UV irradiation and detection of GFP-XRCC1 with immunofluorescence microscopy was conducted as previously described [27]. Cyclobutane pyrimidine dimer (CPD) induced by UV was detected using anti-CPD polyclonal antibody.

### Partial digestion of chromatin DNA with micrococcal nuclease (MNase)

Partial digestion of chromatin DNA with MNase was performed as described previously [28–30]. Briefly,  $5 \times 10^7$  cells were harvested and suspended well by pipetting in 0.5 ml of lysis buffer (18% Ficoll 400, 10 mM  $\text{KH}_2\text{PO}_4$ , 10 mM  $\text{K}_2\text{HPO}_4$ , 1 mM  $\text{MgCl}_2$ , 0.25 mM EGTA, 0.25 mM EDTA, and complete™ Protease Inhibitor Cocktail [Roche, Mannheim, Germany]). After centrifugation at 14,000 rpm for 30 min at 4°C, the crude nuclear pellet was resuspended in 0.6 ml of buffer A (10 mM Tris-HCl [pH 8.0], 150 mM NaCl, 5 mM KCl, 1 mM EDTA, and 1 mM Pefabloc SC [Roche, Mannheim, Germany]). After addition of  $\text{CaCl}_2$  (5 mM final concentration), 0.1 ml aliquots of crude nuclear suspension were digested with different concentration of MNase (0, 10, and 20 U/ml) at 37°C for 5 min. The reaction was terminated by adding 25 mM EDTA, and the DNA was purified by incubation with 1% SDS and 20  $\mu\text{g}/\text{ml}$  proteinase K (Merck, Darmstadt, Germany) at 55°C, followed by phenol-chloroform extraction.

### Isolation of nuclear-soluble and chromatin-bound fractions from DT40 cells

We isolated the nuclear soluble fraction from DT40 cells using the Subcellular Protein Fractionation Kit for Cultured Cells (Thermo, PA). Histone and Topoisomerase I was detected using following specific antibodies (anti-Histone H3 from MBL, MABI0301 and anti-Topoisomerase I from BD Pharmingen™, 556597).

### Alkaline comet assay

For the chicken DT40 cells, the tail DNA percentage, reflecting the number of SSBs (% DNA in tail) [31], was measured for cells that had been exposed to 25  $\mu\text{M}$   $\text{H}_2\text{O}_2$  for 20 min on ice, and cells that had been exposed to 25  $\mu\text{M}$   $\text{H}_2\text{O}_2$  for 20 min on ice followed by a 30 min repair period at 39.5°C. For DT40 cells, a Comet Analysis System was used to quantify the comet tails (Comet 3.0, Kinetic Imaging Ltd., Liverpool, UK). Human TK6 cells were treated with 80  $\mu\text{M}$   $\text{H}_2\text{O}_2$  on ice for 30 min or with MMS at 37°C for 15 min and subsequently released in drug-free, pre-warmed culture medium. Alkaline-comet and single-cell gel electrophoresis assays were performed as described previously [14, 15, 32]. Electrophoresis was carried out by applying 25 volts at 4°C for 50 min using a submarine gel electrophoresis machine (Cat. NB-1012, NIHON EIDO CO. Ltd.) filled with 1850 ml running buffer (0.3 M NaOH, 1 mM EDTA). For TK6 cells, a Comet Analysis System was used to quantify the comet tails (Comet analyzer, YOUWORKS CO. Ltd.). 100 cells were scored per sample.

## Alkaline elution assay

The number of SSBs was quantified using the alkaline elution assay, as described previously [33, 34]. Chicken DT40 cells were radiolabeled with [<sup>14</sup>C] thymidine (0.01–0.02 μCi/ml) for 16 h, chased in radioisotope-free medium for 4 h, followed by H<sub>2</sub>O<sub>2</sub> treatment. Alkaline elution was then carried out under deproteinizing, DNA-denaturing conditions, and fractions were collected into scintillation vials at 180 min intervals. Radioactivity in each fraction was analyzed with a liquid scintillation analyzer (Packard Instruments, Meriden, CT).

## Results

### *ALC1*<sup>-/-</sup> DT40 cells are hypersensitive to H<sub>2</sub>O<sub>2</sub> and MMS

We disrupted the *ALC1* gene in the chicken DT40 line (panel A, B in S1 Fig) and found that the resulting *ALC1*<sup>-/-</sup> cells proliferated with normal kinetics (Fig 1A) and showed a normal cell-cycle distribution (panel C in S1 Fig). To investigate the role played by ALC1 in BER, we measured sensitivity to H<sub>2</sub>O<sub>2</sub> and MMS [35, 36]. The *ALC1*<sup>-/-</sup> cells were hypersensitive to H<sub>2</sub>O<sub>2</sub> and MMS, as were the *PARP1*<sup>-/-</sup> cells (Fig 1B). To learn more about ALC1 as a chromatin-remodeling factor, we inactivated ATPase activity by mutating the essential E165 to Q (the equivalent mutation used in [6, 37]) of the endogenous wild-type *ALC1* allelic gene in *ALC1*<sup>+/+</sup> cells (Fig 1C and S1D Fig). The

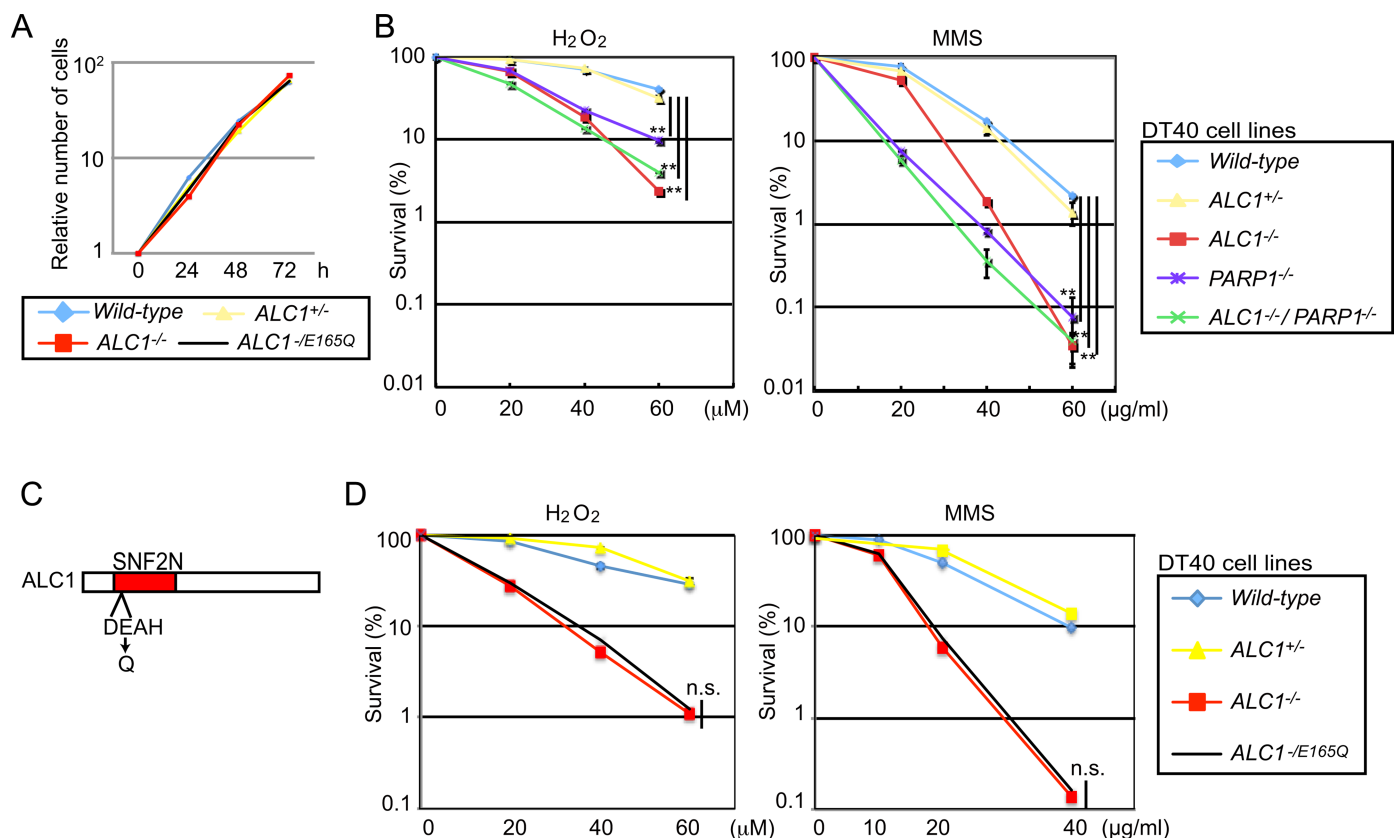


**Fig 1. The *ALC1*<sup>-/-</sup> mutation is epistatic to the *PARP1*<sup>-/-</sup> mutation in DT40-cell sensitivity to H<sub>2</sub>O<sub>2</sub> and MMS.** (A) Growth curves corresponding to the indicated cell cultures. (B) DT40 cells of the indicated genotypes were exposed to H<sub>2</sub>O<sub>2</sub> and methyl methanesulfonate (MMS). The dose of the genotoxic agent is displayed on the x-axis on a linear scale, while the percent fraction of surviving cells is displayed on the y-axis on a logarithmic scale. Error bars represent standard deviations for more than three experiments. (C) Schematic of the SNF2N domain in ALC1. The amino acid change in *ALC1*<sup>-/-E165Q</sup> cells is shown below. (D) The sensitivity of *ALC1*<sup>-/-</sup> and *ALC1*<sup>-/-E165Q</sup> DT40 cells to H<sub>2</sub>O<sub>2</sub> and MMS was very similar. Data as in B. *p*-value was calculated by a student's *t*-test: *p* (\*\*) < 0.01 and n.s. (not significant).

<https://doi.org/10.1371/journal.pone.0188320.g001>

resulting *ALC1*<sup>-E165Q</sup> and *ALC1*<sup>-/-</sup> cells displayed virtually the same phenotype (Fig 1A and 1D), suggesting that ALC1 may promote DNA repair as a chromatin remodeler.

## Epistatic relationship between ALC1 and PARP1 in cellular tolerance to H<sub>2</sub>O<sub>2</sub> and MMS

To analyze the functional relationship between ALC1 and PARP1, we disrupted the *ALC1* gene in *PARP1*<sup>-/-</sup> DT40 cells, generating *ALC1*<sup>-/-</sup>/*PARP1*<sup>-/-</sup> cells. We then analyzed cellular sensitivity to H<sub>2</sub>O<sub>2</sub> and MMS by comparing *wild-type*, *PARP1*<sup>-/-</sup>, *ALC1*<sup>-/-</sup>, and *ALC1*<sup>-/-</sup>/*PARP1*<sup>-/-</sup> clones.

While sensitivity to H<sub>2</sub>O<sub>2</sub> was higher in the *ALC1*<sup>-/-</sup> DT40 cells than in the *PARP1*<sup>-/-</sup> clones, it was very similar in the *ALC1*<sup>-/-</sup> and *ALC1*<sup>-/-</sup>/*PARP1*<sup>-/-</sup> clones (Fig 1B), indicating an epistatic relationship between ALC1 and PARP1. The *ALC1*<sup>-/-</sup> cells, on the other hand, were slightly less sensitive to MMS than were the *PARP1*<sup>-/-</sup> clones. Nonetheless, ALC1 and PARP1 do have an epistatic relationship, as sensitivity to MMS was very similar for the *PARP1*<sup>-/-</sup> and *ALC1*<sup>-/-</sup>/*PARP1*<sup>-/-</sup> clones (Fig 1B). These observations indicate that ALC1's role in cellular tolerance to H<sub>2</sub>O<sub>2</sub> and MMS depends at least partially on the functionality of PARP1. In conclusion, given that PARP1 contributes to H<sub>2</sub>O<sub>2</sub> and MMS tolerance by promoting BER, ALC1 may play a role in BER in the chicken DT40 cell line.

## The important role of ALC1 in BER

The above data suggest that ALC1 may facilitate BER. We thus monitored ongoing BER by measuring the number of SSBs, which are BER intermediates, after a 20 min H<sub>2</sub>O<sub>2</sub> treatment on ice [14, 15]. We then performed the alkaline-comet (Fig 2A) and alkaline-elusion assays (Fig 2B). Immediately after H<sub>2</sub>O<sub>2</sub> pulse-treatment, tail sizes in *wild-type* and *ALC1*<sup>-/-</sup> cells were very similar (Fig 2A). At 30 min after treatment, tails in the *wild-type* cells had decreased to nearly normal size, while tails in the *ALC1*<sup>-/-</sup> cells were significantly longer. Likewise, alkaline elusion showed that 30 min after treatment, *wild-type*, but not *ALC1*<sup>-/-</sup> cells, had eliminated the vast majority of SSBs (Fig 2B). Importantly, the *ALC1*<sup>-/-</sup>, *PARP1*<sup>-/-</sup>, and *ALC1*<sup>-/-</sup>/*PARP1*<sup>-/-</sup> clones all showed similar kinetics in SSB repair in both assays (Fig 2A and 2B). These data demonstrate that ALC1 and PARP1 collaborate in SSB repair in chicken DT40 cells.

To examine ALC1's role in BER in human cells, we created *ALC1*<sup>-/-</sup> clones from the human TK6 cell line (S2 Fig) and analyzed SSB-repair kinetics by performing an alkaline-comet assay in *wild-type* and *ALC1*<sup>-/-</sup> TK6 cells. The *ALC1*<sup>-/-</sup> TK6 cells were more sensitive to MMS than were the *wild-type* cells (Fig 3A). Unlike the DT40 cells, the *ALC1*<sup>-/-</sup> TK6 cells showed similar H<sub>2</sub>O<sub>2</sub> sensitivity compared to *wild-type* (Fig 3A). It is possible that the oxidative stress decreased cellular viability through mechanisms other than DNA damage in this cell line. Nonetheless, delayed SSB repair at 5 min following pulse-exposure to H<sub>2</sub>O<sub>2</sub> was reproducibly seen in the *ALC1*<sup>-/-</sup> TK6 cells (Fig 3B). Moreover, when the pulse-exposed cells were subsequently treated with the chemotherapeutic PARP poison, olaparib, which stabilizes the PARP-DNA complex, the delay in SSB repair in the *ALC1*<sup>-/-</sup> TK6 cells was more pronounced than in the *wild-type* cells [38] (Fig 3C). We thus conclude that ALC1 contributes to SSB repair in the human cell line as well as in the chicken DT40 cells. We examined the kinetics of BER following pulse-exposure to MMS. Note that pulse-exposure to MMS has to be done at 37°C, at which temperature base damage and repair occur in parallel. Alkaline-comet tails were longer in *ALC1*<sup>-/-</sup> than in *wild-type* cells after pulse-exposure to MMS (S3 Fig), suggesting a BER defect in the *ALC1*<sup>-/-</sup> cells. To examine the actual BER kinetics, we pulse-exposed *wild-type* and *ALC1*<sup>-/-</sup> cells to MMS and released in drug-free medium. Repair in the *ALC1*<sup>-/-</sup> cells was significantly delayed during the chase period (Fig 3D). We thus conclude that ALC1 promotes BER in both chicken DT40 and human TK6 cell lines.

## ALC1 is dispensable for the recruitment of XRCC1 to damage sites

Having confirmed that ALC1 and PARP1 have an epistatic relationship in BER in chicken DT40 cells, we next attempted to define the role played by ALC1 in the promotion of BER by PARP. To determine whether or not ALC1 controls PARP-mediated PARylation, we measured intracellular NAD(P)H during continuous exposure to H<sub>2</sub>O<sub>2</sub> and MMS [26, 27, 39, 40].

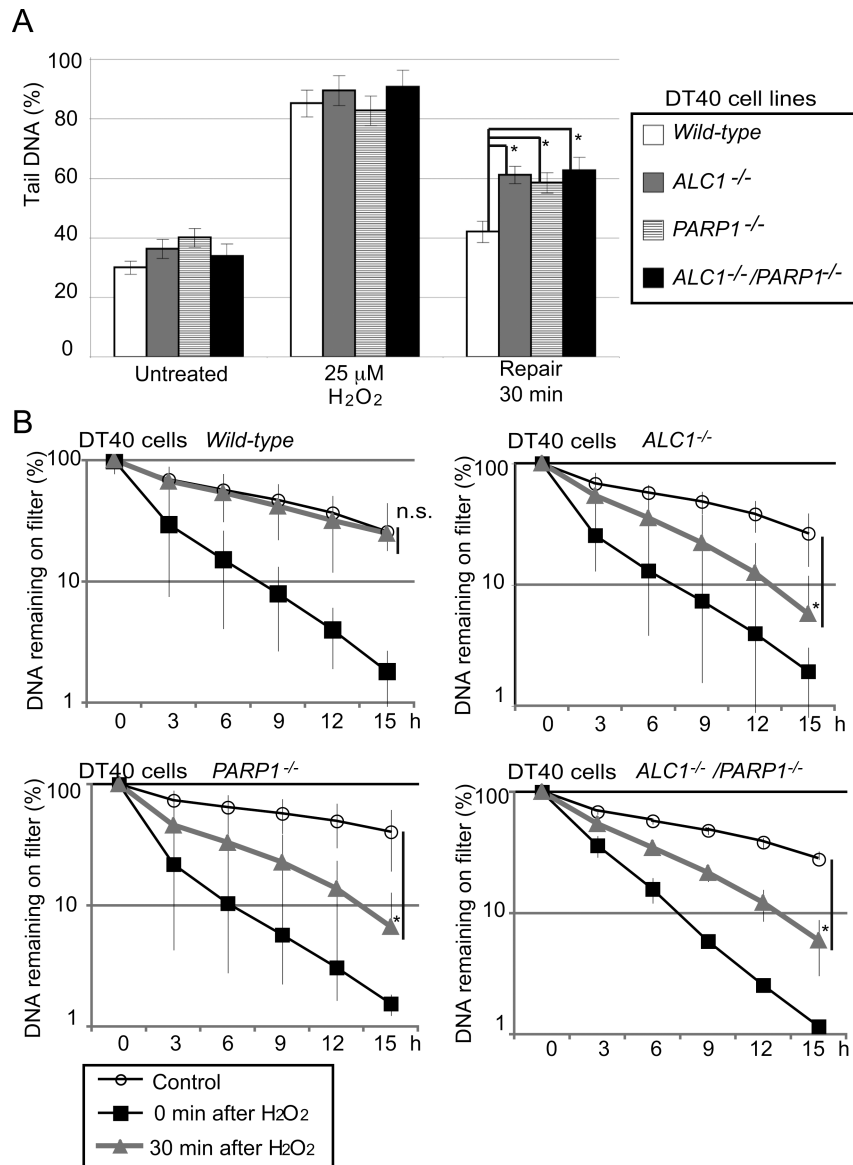


**Fig 2. ALC1 is required for the repair of SSBs, which are BER intermediates, in DT40 cells.** (A) Alkaline-comet assay to detect SSBs. Indicated genotype were tested in untreated cells, immediately after exposure to 25 μM H<sub>2</sub>O<sub>2</sub> on ice, and after a further 30 min incubation (repair period). Error bars represent standard deviations from three independent experiments. Tail-DNA percentage, defined as percentage of damaged DNA (% DNA in tail), was calculated as described in Materials and Methods. Tail-DNA % is displayed on the y-axis on a linear scale. (B) Alkaline elution experiment to detect SSB frequency. The data are expressed as the fraction of DNA remaining on the filter for the indicated genotypes of untreated cells (white circle), pulse H<sub>2</sub>O<sub>2</sub>-treated cells (black square), and the H<sub>2</sub>O<sub>2</sub>-treated cells incubated for a further 30 min (gray triangle). Elution time is displayed on the x-axis on a linear scale. The percentage of DNA remaining on the filter is displayed on the y-axis on a logarithmic scale. Error bars represent standard deviations from three independent experiments. *p*-value was calculated by a student's *t*-test: *p* (\*) <0.05, and n.s. (not significant).

<https://doi.org/10.1371/journal.pone.0188320.g002>



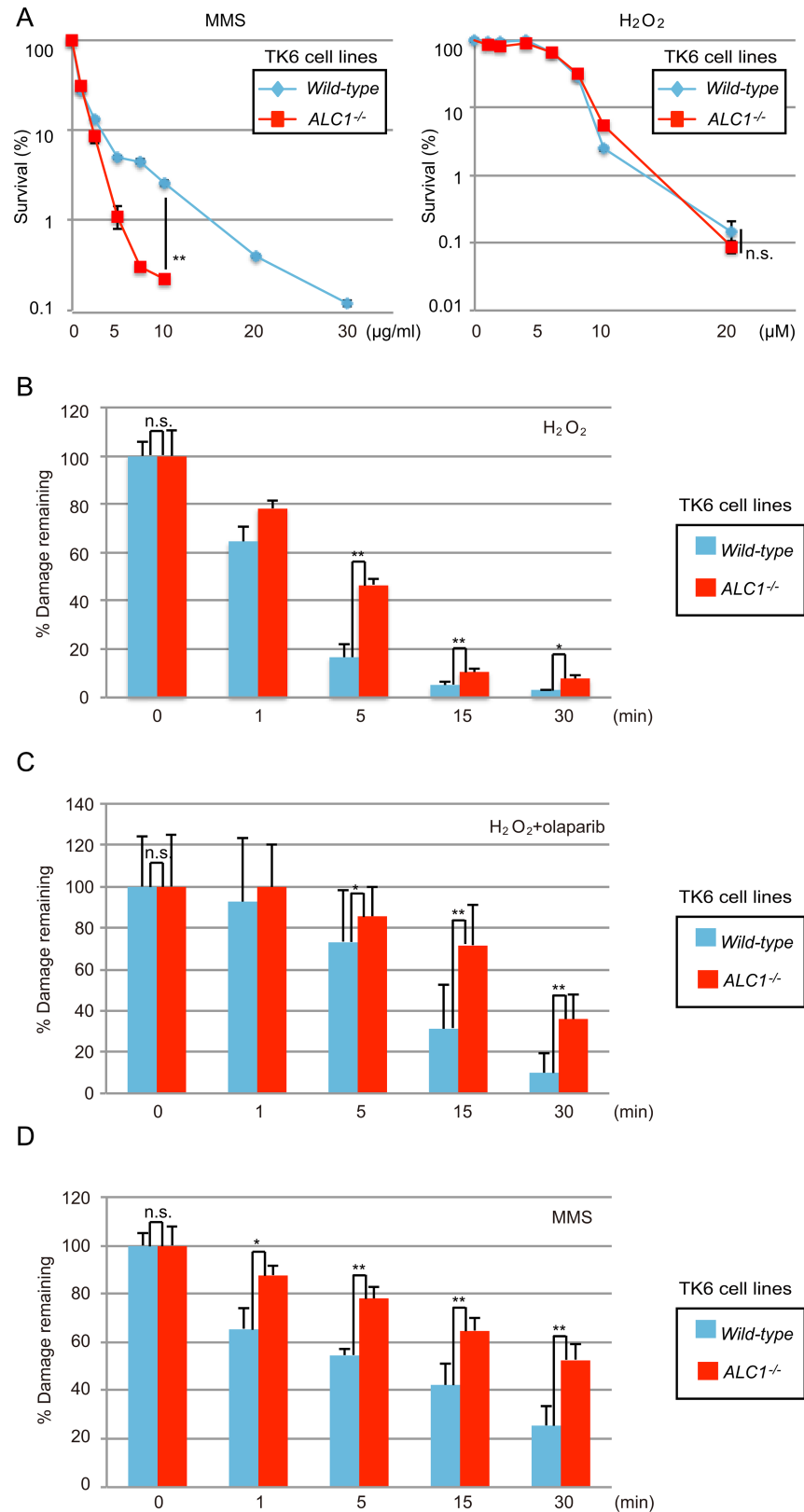


**Fig 3. ALC1 is required for the repair of SSBs, which are BER intermediates, in human TK6 cells.** (A) DNA-damage sensitivity of TK6 cells carrying the indicated genotype. Data as in Fig 1B. (B–D) Alkaline-comet assay to detect unrepaired SSBs in human TK6 cells. The percentage of DNA strand breaks remaining at the indicated time points is displayed on the y-axis on a linear scale. Error bars represent standard deviations

from three independent experiments. (B) Human TK6 cells of the indicated genotype were exposed to 80  $\mu\text{M}$   $\text{H}_2\text{O}_2$  on ice for 30 min. The cells were released in drug-free, pre-warmed culture medium and further cultured for the indicated time. (C) TK6 cells treated with  $\text{H}_2\text{O}_2$  as in B were released in culture medium containing 1  $\mu\text{M}$  olaparib then cultured for the indicated time. (D) *Wild-type* and *ALC1*<sup>-/-</sup> TK6 cells were treated with 0.1 and 0.075 mg/ml MMS, respectively, for 15 min. Cells were then released in drug-free, pre-warmed culture medium and further cultured for indicated time. *p*-value was calculated by a student's *t*-test: *p* (\*\*) <0.01, (\*) <0.05, and n.s. (not significant).

<https://doi.org/10.1371/journal.pone.0188320.g003>

This assay monitors PARP-mediated PARylation, since reduction of  $\text{NAD}^+$ , a major substrate of PARP, results in depletion of cellular  $\text{NAD(P)H}$  [26]. We found that the amount of  $\text{NAD(P)H}$  was reduced in *wild-type* and *ALC1*<sup>-/-</sup> DT40 cells with very similar kinetics (Fig 4A), indicating that PARylation occurs normally in *ALC1*<sup>-/-</sup> cells [38].

We considered that ALC1 might control PARP-mediated recruitment of XRCC1 to damage sites. To test this hypothesis, we induced SSBs selectively in subnuclear areas and examined the kinetics of XRCC1 relocation to SSB sites [42]. To induce SSBs, we employed a nucleotide-excision, repair-deficient xeroderma pigmentosum group A (XPA) U2OS cells expressing *Neurospora crassa* UV-damage endonuclease (UVDE), which generates SSBs at UV

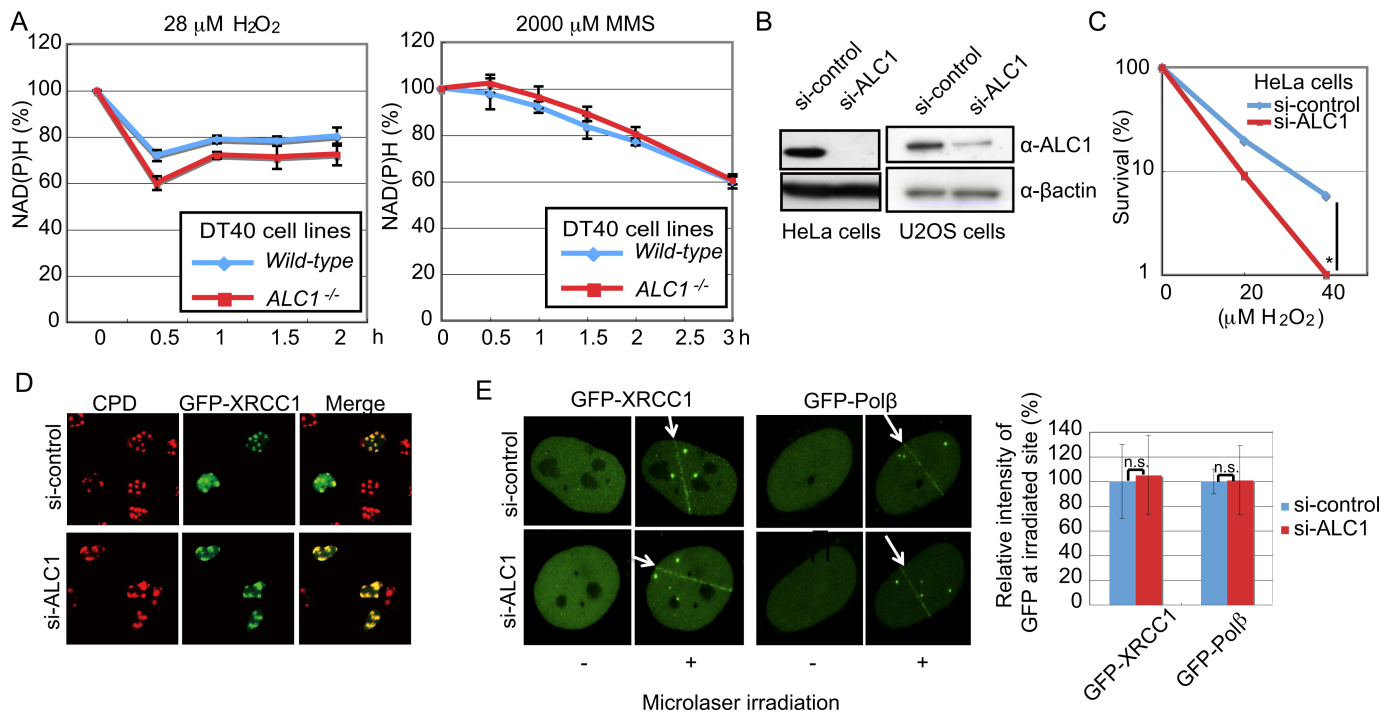


**Fig 4. ALC1 is not required for PARylation or recruitment of Pol $\beta$  or XRCC1 to DNA-damage sites.** (A) DT40 clones of the indicated genotypes were treated with  $\text{H}_2\text{O}_2$  or MMS and harvested at the indicated times after treatment. To evaluate the activation of the PARylation event by PARP1 at SSB sites, we measured the cellular concentration of  $\text{NAD(P)H}$ , the major substrate for PARP. Time after treatment with  $\text{H}_2\text{O}_2$  or MMS is displayed on the x-axis, while the relative cellular  $\text{NAD(P)H}$  concentration is displayed on the y-axis. (B) Knockdown of ALC1 using si-RNA in human HeLa and U2OS cells was verified by western blot analysis using anti-ALC1 and anti- $\beta$ -actin (loading control). (C)  $\text{H}_2\text{O}_2$  sensitivity of ALC1-depleted or control si-RNA-treated HeLa cells. The dose of  $\text{H}_2\text{O}_2$  is displayed on the x-axis on a linear scale, while the percentage of cell survival is displayed on the y-axis on a logarithmic scale. (D) U2OS cells deficient in nucleotide excision repair, xeroderma pigmentosum group A<sup>-</sup> (XPA<sup>-</sup>) expressing *Neurospora crassa* UV-damage endonuclease (UVDE) were exposed to 100  $\text{J}/\text{m}^2$  UV through micro pores in membrane filters. DNA single-strand breaks were produced at UV-irradiated region, where GFP-XRCC1 accumulated independently of ALC1 expression. Representative image of XPA-UVDE cells displaying GFP-XRCC1 and UV damage (CPD) signals. (E) GFP-XRCC1 and GFP-Pol $\beta$  accumulate immediately at DNA damage sites after exposure to a 405 nm pulse laser in U2OS cells, which have been treated with siRNA against ALC1 or control siRNA for 48 h as previously described [41]. GFP-signal intensity for GFP-XRCC1 and GFP-Pol $\beta$  is displayed in the histogram. Error bars represent standard deviations from three independent experiments. *p*-value was calculated by a student's *t*-test: *p* (\*) <0.05, and n.s. (not significant).

<https://doi.org/10.1371/journal.pone.0188320.g004>

photoproducts [27, 43]. We depleted ALC1 using si-RNA in HeLa and U2OS cells (Fig 4B) and monitored the recruitment of BER factors to induced SSB sites after UV irradiation. As with the *ALC1*<sup>-/-</sup> DT40 cells (Fig 1), the ALC1-depleted HeLa cells showed a higher sensitivity to H<sub>2</sub>O<sub>2</sub> than did the si-control-RNA-treated cells (Fig 4C). On the other hand, the depletion of ALC1 did not impair the recruitment of XRCC1 to induced SSB sites (Fig 4D). Similarly, GFP-XRCC1 was efficiently recruited to laser-induced DNA damage sites in ALC1-depleted and control cells (Fig 4E). Moreover, recruited XRCC1 seemed to be functional, since GFP-Polβ also accumulated at DNA-damage sites (Fig 4E). We thus conclude that ALC1 contributes to BER independently of XRCC1.

### ALC1 facilitates BER by relaxing chromatin at DNA-damage sites

The above conclusion led us to consider that ALC1 might promote chromatin relaxation at DNA-damage sites to facilitate DNA repair. To monitor the extent of chromatin compaction, we performed the MNase chromatin digestion assay. We exposed chicken DT40 cells to H<sub>2</sub>O<sub>2</sub>, then partially digested chromatin DNA with MNase, and quantified the fraction of the mononucleosome. Five min after treatment with 5 mM H<sub>2</sub>O<sub>2</sub>, the amount of partially digested product, ~146 bp DNA (Fig 5A, box), was significantly increased in *wild-type* cells (Fig 5A, lanes 1, 2 and 3, 4), but not in *ALC1*<sup>-/-</sup> cells (Fig 5A, lanes 5, 6 and 7, 8). The data suggest that configuration of chromatin changes into open status in *wild-type* but not in *ALC1*<sup>-/-</sup> cells by DNA-damage presumably through inducing histone eviction (Fig 5A). To further examine this possibility, we measured the amount of histone H3 released from the chromatin after DNA damage (Fig 5B). The amount of histone H3 in the nuclear soluble fraction was increased in *wild-type* cells after H<sub>2</sub>O<sub>2</sub> treatment, suggesting that DNA-damage induces histone eviction from chromatin (Fig 5B). However, such histone eviction was reduced in *ALC1*<sup>-/-</sup> cells (Fig 5B). These results suggest that ALC1 promotes BER by inducing chromatin remodeling through histone eviction and facilitating the access of BER factors to DNA-damage sites.

### The *ALC1* locus is unstable and susceptible to gene amplification in a large number of malignant tumors

Overexpression as well as depletion of ALC1 sensitizes cells to DNA-damaging agents [11], suggesting that maintaining a proper expression level of the cellular ALC1 protein is important for effective responses to DNA damage. We surveyed ~1,000 cancer-cell lines registered in the Cancer Cell Line Encyclopedia [44]. Surprisingly, the *ALC1* gene was amplified in a majority of the cell lines (Fig 6A), indicating that the *ALC1* locus may be extremely unstable and susceptible to gene amplification. The expression level of ALC1 significantly correlates with that of PARP1 (Fig 6B), but the molecular mechanisms underlying this correlation remain unclear. One possible scenario is that toxic effects caused by overexpression of ALC1 might be suppressed by simultaneous upregulation of PARP1. The correlation also supports the idea that appropriate control of ALC1 expression contributes to genome maintenance of malignant cells.

### Discussion

During the past decade, roles played by ALC1 in the regulation DNA repair as well as its PARP1 stimulated chromatin-repositioning enzyme activity have been well determined [6, 10, 11, 37, 45, 46]. In this study, we explored ALC1's possible role in BER in the chicken DT40 and human TK6 cell lines. Alkaline-comet and alkaline-elusion assays consistently showed that ALC1 promotes BER a step after SSB formation in both chicken and human cells (Figs 2 and 3). These results were consistent with the previously suggested possible roles of ALC1 in DNA

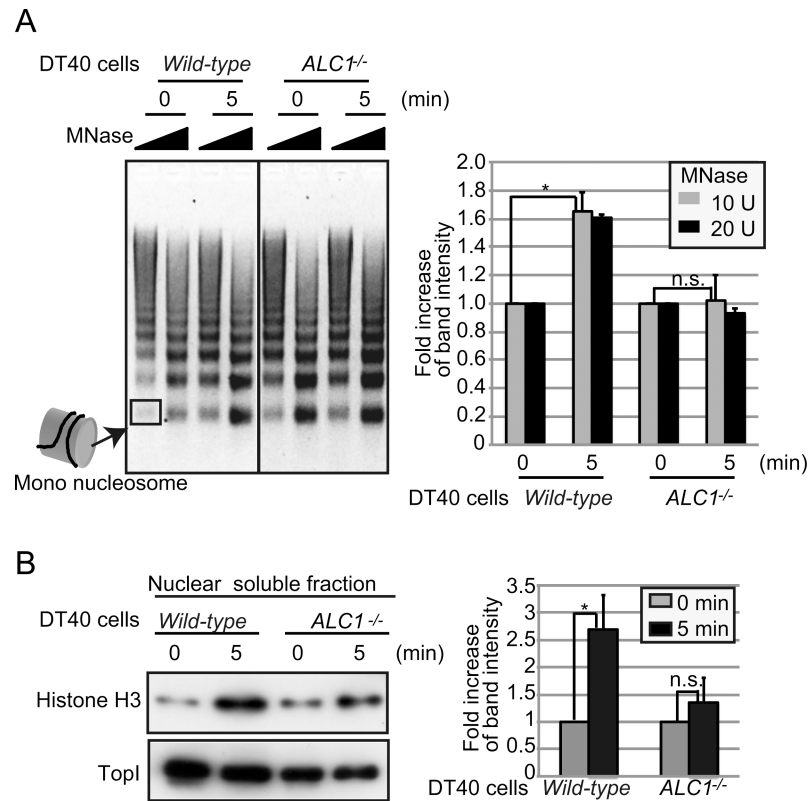


**Fig 5. ALC1 facilitates DNA-damage-induced chromatin relaxation.** (A) DT40 cells of the indicated genotypes were treated with H<sub>2</sub>O<sub>2</sub>, and cells were harvested at the indicated times after H<sub>2</sub>O<sub>2</sub> treatment. The chromatin fraction was digested with 10 and 20 U/ml MNase. Digested genomic DNA products were analyzed by gel electrophoresis. The relative intensity of the band corresponding to the mono-nucleosome (146 bp, indicated by arrow) was quantified. (B) Histone H3 present in the nuclear soluble fraction was detected by western blot. The blot was probed with anti-Topoisomerase I (Top1) antibody as a loading control. The relative intensity of the band corresponding to histone H3 was quantified and normalized for the level of Top1. *p*-value was calculated by a student's *t*-test: *p* (\*) <0.05, and n.s. (not significant).

<https://doi.org/10.1371/journal.pone.0188320.g005>

repair [6, 46]. We also demonstrated the epistatic relationship between ALC1<sup>-/-</sup> and PARP1<sup>-/-</sup> mutations in cellular resistance to H<sub>2</sub>O<sub>2</sub> and MMS in chicken DT40 cells (Fig 1). The epistatic relationship between ALC1<sup>-/-</sup> and PARP1<sup>-/-</sup> is consistent with the previous reports showing that ALC1 is recruited to the site of DNA damage and activated through PARylation [6, 37, 45]. Since PARP1 plays a role in BER, this epistatic relationship further supports the conclusion that ALC1 plays a role in BER. We thus conclude that ALC1 significantly promotes BER.

The higher sensitivity to H<sub>2</sub>O<sub>2</sub> found in ALC1<sup>-/-</sup> DT40 cells compared to PARP1<sup>-/-</sup> DT40 cells (Fig 1) reveals the critical role of ALC1 in cellular tolerance to oxidative DNA damage. This observation is very surprising, because the promotion of SSB repair by PARylation has previously been attributed solely to the enhanced recruitment of XRCC1 to DNA-damage sites by PARP. Our data reveal that ALC1 contributes to the PARP-dependent promotion of BER without affecting the recruitment of XRCC1 or Polβ to DNA lesions (Fig 4). We thus conclude that ALC1 plays a key role in SSB repair, independent of both XRCC1 and Polβ (Fig 4).

An important question is, how does ALC1 contribute to BER? A significant delay in the repair of SSBs, which are BER intermediates (Figs 2 and 3), indicates that ALC1 contributes to promoting the sealing of SSBs. ALC1 facilitates chromatin relaxation, most likely at DNA-damage sites (Fig 5). This is consistent with the fact that attenuation of ALC1's ATPase activity by the E165Q mutation completely inactivates its functions (Fig 1) [6, 37]. One possible

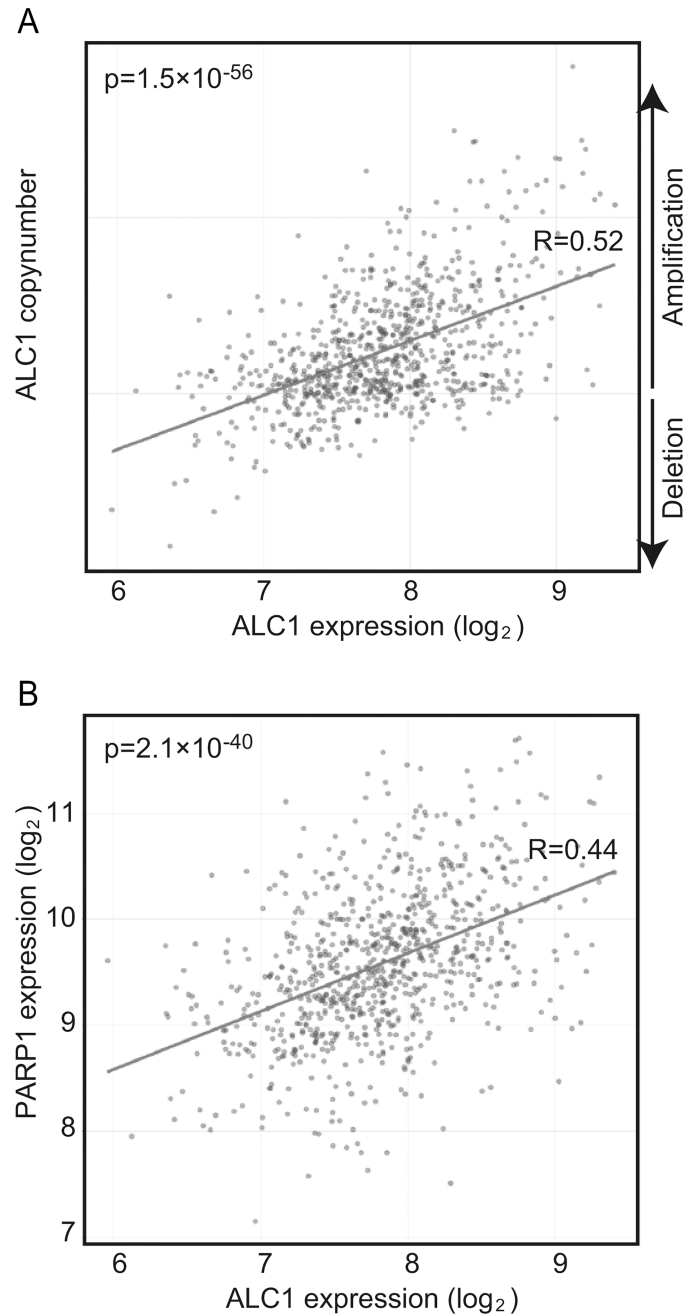


**Fig 6. Overexpression of *ALC1* in a wide variety of cancer cell lines.** (A) Transcriptional characteristics of *ALC1* were surveyed in 1000 cancer-cell lines using the Cancer Cell Line Encyclopedia [44]. The relative expression level of *ALC1* in the cancer-cell lines is displayed on the x-axis on a logarithmic scale, while the relative copy number of the *ALC1* gene is displayed on the y-axis on a linear scale. (B) Relationship between *ALC1* and *PARP1* expression levels in 1000 cancer cell lines. The relative expression of *ALC1* is displayed on the x-axis, while the relative expression of *PARP1* is displayed on the y-axis on a logarithmic scale. R-value represents correlation coefficients. p-value was calculated by t-test.

<https://doi.org/10.1371/journal.pone.0188320.g006>

scenario is that chromatin remodeling by *ALC1* might facilitate long-patch repair by removing nucleosomes for DNA-repair synthesis by DNA polymerases  $\beta$  and  $\delta$ . Future research is indicated to clarify *ALC1*'s role in BER by conducting *in vitro* BER in a chromatin context.

## Supporting information

**S1 Fig. Generation of  $ALC1^{-/-}$  cells from chicken DT40 cells.** (A) Schematic showing part of the *GdALC1* locus. The filled boxes represent exons. The thick lines show the genomic region amplified for the targeting-vector arms. The relevant *ScaI* and *BamHI* sites and the position of the probe used for Southern blot analysis are indicated. (B) Southern blot analysis of *wild-type* (+/+), heterozygous mutant (+/-), and homozygous mutant (-/-). *ScaI*- and *BamHI*-digested genomic DNA was hybridized with the probe shown in (A). (C) Representative cell-cycle distribution of the indicated cell cultures as measured by BrdU incorporation and DNA content in flow-cytometric analysis. The upper, lower left, lower right, and leftmost gates correspond to cells in the S, G1, and G2/M phases, and sub-G1 fraction, respectively. Numbers show the percentage of cells that fall within each gate. (D) Generation of the ALC1-ATPase-deficient  $ALC1^{-/E165Q}$  clone. Schematic showing part of the *GdALC1* locus. The filled boxes represent exons. The thick lines show the genomic region amplified for the targeting-vector arms. The relevant *BamHI* site and the position of the probe used for Southern blot are indicated. (PDF)

**S2 Fig. Disruption of *ALC1* gene in human TK6 cells.** (A) Schematic of part of the human *ALC1* locus. The knockout constructs are shown below the locus. The filled boxes represent exons. The thick lines show the genomic region amplified for targeting-vector arms. (B) *Wild-type* (+/+) as well as  $ALC1^{-/-}$  (-/-) TK6 cells were subjected to RT-PCR using *GAPDH*- or *ALC1*-specific primers. (C) *Wild-type* (+/+) as well as  $ALC1^{-/-}$  (-/-) TK6 cells were subjected to western blot using  $\alpha$ -ALC1 specific antibody. The blot was probed with  $\alpha$ - $\beta$ actin antibody as a loading control. (PDF)

**S3 Fig. The accumulation of MMS-induced SSBs in the  $ALC1^{-/-}$  human TK6 cells.** The average of the median of tail moments from 100 comets in each assay is displayed on the y-axis on a linear scale. Error bars represent standard deviations from three independent experiments. Indicated TK6 cells were treated with indicated concentrations of MMS at 37°C for 15 min. In this condition, base damage and repair occur in parallel. (PDF)

## Acknowledgments

We would like to thank the Radioisotope Research Center in Kyoto University and Tokyo Metropolitan University for support in the use of isotopes. The authors thank K. Kadoda for setting up alkaline comet assay and the members of the Department of Radiation Genetics for their comments.

## Author Contributions

**Data curation:** Akira Yasui, Tomoo Ogi, Yves Pommier, Kouji Hirota.

**Investigation:** Masataka Tsuda, Kosai Cho, Masato Ooka, Naoto Shimizu, Reiko Watanabe, Yuka Nakazawa, Hiroshi Harada, Keli Agama, Jun Nakamura, Ryuta Asada, Haruna Fujiike, Tetsushi Sakuma, Junko Murai, Masahiro Hiraoka, Kaoru Koike, Kouji Hirota.

**Methodology:** Takashi Yamamoto.

**Supervision:** Shunichi Takeda, Kouji Hirota.

**Writing – original draft:** Masataka Tsuda, Kouji Hirota.

Writing – review & editing: Yves Pommier, Shunichi Takeda, Kouji Hirota.

## References

- Abbotts R, Wilson DM 3rd. Coordination of DNA single strand break repair. *Free Radic Biol Med*. 2016. <https://doi.org/10.1016/j.freeradbiomed.2016.11.039> PMID: 27890643.
- Robertson AB, Klungland A, Rognes T, Leiros I. DNA repair in mammalian cells: Base excision repair: the long and short of it. *Cell Mol Life Sci*. 2009; 66(6):981–93. Epub 2009/01/21. <https://doi.org/10.1007/s00018-009-8736-z> PMID: 19153658.
- Caldecott KW. Single-strand break repair and genetic disease. *Nat Rev Genet*. 2008; 9(8):619–31. Epub 2008/07/16. doi: nrg2380 [pii] <https://doi.org/10.1038/nrg2380> PMID: 18626472.
- Hanzlikova H, Gittens W, Krejciikova K, Zeng Z, Caldecott KW. Overlapping roles for PARP1 and PARP2 in the recruitment of endogenous XRCC1 and PNKP into oxidized chromatin. *Nucleic Acids Res*. 2016. <https://doi.org/10.1093/nar/gkw1246> PMID: 27965414.
- Karras GI, Kustatscher G, Buhecha HR, Allen MD, Pugieux C, Sait F, et al. The macro domain is an ADP-ribose binding module. *EMBO J*. 2005; 24(11):1911–20. Epub 2005/05/20. doi: 7600664 [pii] <https://doi.org/10.1038/sj.emboj.7600664> PMID: 15902274; PubMed Central PMCID: PMC1142602.
- Ahel D, Horejsi Z, Wiechens N, Polo SE, Garcia-Wilson E, Ahel I, et al. Poly(ADP-ribose)-dependent regulation of DNA repair by the chromatin remodeling enzyme ALC1. *Science*. 2009; 325(5945):1240–3. Epub 2009/08/08. doi: 1177321 [pii] <https://doi.org/10.1126/science.1177321> PMID: 19661379.
- Eisen JA, Sweder KS, Hanawalt PC. Evolution of the SNF2 family of proteins: subfamilies with distinct sequences and functions. *Nucleic Acids Res*. 1995; 23(14):2715–23. Epub 1995/07/25. doi: 5a0167 [pii]. PMID: 7651832; PubMed Central PMCID: PMC307096.
- Flaus A, Martin DM, Barton GJ, Owen-Hughes T. Identification of multiple distinct Snf2 subfamilies with conserved structural motifs. *Nucleic Acids Res*. 2006; 34(10):2887–905. Epub 2006/06/02. doi: 34/10/2887 [pii] <https://doi.org/10.1093/nar/gkl295> PMID: 16738128; PubMed Central PMCID: PMC1474054.
- Gorbalenya AE, Koonin EV, Donchenko AP, Blinov VM. Two related superfamilies of putative helicases involved in replication, recombination, repair and expression of DNA and RNA genomes. *Nucleic Acids Res*. 1989; 17(12):4713–30. Epub 1989/06/26. PMID: 2546125; PubMed Central PMCID: PMC318027.
- Pines A, Vrouwe MG, Martijn JA, Typas D, Luijsterburg MS, Cansoy M, et al. PARP1 promotes nucleotide excision repair through DDB2 stabilization and recruitment of ALC1. *J Cell Biol*. 2012; 199(2):235–49. <https://doi.org/10.1083/jcb.201112132> PMID: 23045548; PubMed Central PMCID: PMCPMC3471223.
- Kulkarni A, Oza J, Yao M, Sohail H, Ginjala V, Tomas-Loba A, et al. Tripartite Motif-containing 33 (TRIM33) protein functions in the poly(ADP-ribose) polymerase (PARP)-dependent DNA damage response through interaction with Amplified in Liver Cancer 1 (ALC1) protein. *J Biol Chem*. 2013; 288(45):32357–69. <https://doi.org/10.1074/jbc.M113.459164> PMID: 23926104; PubMed Central PMCID: PMCPMC3820871.
- Ball LG, Xiao W. Molecular basis of ataxia telangiectasia and related diseases. *Acta Pharmacol Sin*. 2005; 26(8):897–907. Epub 2005/07/26. <https://doi.org/10.1111/j.1745-7254.2005.00165.x> PMID: 16038621.
- Pachkowski BF, Tano K, Afonin V, Elder RH, Takeda S, Watanabe M, et al. Cells deficient in PARP-1 show an accelerated accumulation of DNA single strand breaks, but not AP sites, over the PARP-1-proficient cells exposed to MMS. *Mutat Res*. 2009; 671(1–2):93–9. <https://doi.org/10.1016/j.mrfmmm.2009.09.006> PMID: 19778542; PubMed Central PMCID: PMCPMC2784157.
- El-Khamisy SF, Saifi GM, Weinfeld M, Johansson F, Helleday T, Lupski JR, et al. Defective DNA single-strand break repair in spinocerebellar ataxia with axonal neuropathy-1. *Nature*. 2005; 434(7029):108–13. <https://doi.org/10.1038/nature03314> PMID: 15744309.
- Hoch NC, Hanzlikova H, Rulten SL, Tetreault M, Komulainen E, Ju L, et al. XRCC1 mutation is associated with PARP1 hyperactivation and cerebellar ataxia. *Nature*. 2017; 541(7635):87–91. <https://doi.org/10.1038/nature20790> PMID: 28002403; PubMed Central PMCID: PMCPMC5218588.
- Buerstedde JM, Takeda S. Increased ratio of targeted to random integration after transfection of chicken B cell lines. *Cell*. 1991; 67(1):179–88. PMID: 1913816.
- Hirota K, Sonoda E, Kawamoto T, Motegi A, Masutani C, Hanaoka F, et al. Simultaneous disruption of two DNA polymerases, Poleta and Polzeta, in Avian DT40 cells unmasks the role of Poleta in cellular response to various DNA lesions. *PLoS Genet*. 2010; 6(10). <https://doi.org/10.1371/journal.pgen.1001151> PMID: 20949111; PubMed Central PMCID: PMC2951353.
- Fujita M, Sasanuma H, Yamamoto KN, Harada H, Kurosawa A, Adachi N, et al. Interference in DNA replication can cause mitotic chromosomal breakage unassociated with double-strand breaks. *PLoS*

- One. 2013; 8(4):e60043. <https://doi.org/10.1371/journal.pone.0060043> PMID: 23573231; PubMed Central PMCID: PMC3616066.
19. Hirota K, Tsuda M, Mohiuddin, Tsurimoto T, Cohen IS, Livneh Z, et al. In vivo evidence for translesion synthesis by the replicative DNA polymerase delta. *Nucleic Acids Res.* 2016; 44(15):7242–50. <https://doi.org/10.1093/nar/gkw439> PMID: 27185888; PubMed Central PMCID: PMC5009730.
  20. Hirota K, Yoshikiyo K, Guilbaud G, Tsurimoto T, Murai J, Tsuda M, et al. The POLD3 subunit of DNA polymerase delta can promote translesion synthesis independently of DNA polymerase zeta. *Nucleic Acids Res.* 2015; 43(3):1671–83. <https://doi.org/10.1093/nar/gkv023> PMID: 25628356; PubMed Central PMCID: PMC4330384.
  21. Levy JA, Virolainen M, Defendi V. Human lymphoblastoid lines from lymph node and spleen. *Cancer.* 1968; 22(3):517–24. PMID: 5673231.
  22. Honma M. Generation of loss of heterozygosity and its dependency on p53 status in human lymphoblastoid cells. *Environ Mol Mutagen.* 2005; 45(2–3):162–76. <https://doi.org/10.1002/em.20113> PMID: 15688360.
  23. Yamamoto KN, Kobayashi S, Tsuda M, Kurumizaka H, Takata M, Kono K, et al. Involvement of SLX4 in interstrand cross-link repair is regulated by the Fanconi anemia pathway. *Proc Natl Acad Sci U S A.* 2011; 108(16):6492–6. <https://doi.org/10.1073/pnas.1018487108> PMID: 21464321; PubMed Central PMCID: PMC3080998.
  24. Saberi A, Hohegger H, Szuts D, Lan L, Yasui A, Sale JE, et al. RAD18 and poly(ADP-ribose) polymerase independently suppress the access of nonhomologous end joining to double-strand breaks and facilitate homologous recombination-mediated repair. *Mol Cell Biol.* 2007; 27(7):2562–71. Epub 2007/01/24. doi: MCB.01243-06 [pii] <https://doi.org/10.1128/MCB.01243-06> PMID: 17242200; PubMed Central PMCID: PMC1899888.
  25. Sakuma T, Ochiai H, Kaneko T, Mashimo T, Tokumasu D, Sakane Y, et al. Repeating pattern of non-RVD variations in DNA-binding modules enhances TALEN activity. *Sci Rep.* 2013; 3:3379. <https://doi.org/10.1038/srep03379> PMID: 24287550; PubMed Central PMCID: PMC3843162.
  26. Nakamura J, Asakura S, Hester SD, de Murcia G, Caldecott KW, Swenberg JA. Quantitation of intracellular NAD(P)H can monitor an imbalance of DNA single strand break repair in base excision repair deficient cells in real time. *Nucleic Acids Res.* 2003; 31(17):e104. Epub 2003/08/22. PubMed <https://doi.org/10.1093/nar/gng105> PMID: 12930978; PubMed Central PMCID: PMC212824.
  27. Okano S, Lan L, Caldecott KW, Mori T, Yasui A. Spatial and temporal cellular responses to single-strand breaks in human cells. *Mol Cell Biol.* 2003; 23(11):3974–81. Epub 2003/05/16. PubMed <https://doi.org/10.1128/MCB.23.11.3974-3981.2003> PMID: 12748298; PubMed Central PMCID: PMC155230.
  28. Asada R, Takemata N, Hoffman CS, Ohta K, Hirota K. Antagonistic controls of chromatin and mRNA start site selection by Tup family corepressors and the CCAAT-binding factor. *Mol Cell Biol.* 2015; 35(5):847–55. <https://doi.org/10.1128/MCB.00924-14> PMID: 25535331; PubMed Central PMCID: PMC4323495.
  29. Hirota K, Miyoshi T, Kugou K, Hoffman CS, Shibata T, Ohta K. Stepwise chromatin remodelling by a cascade of transcription initiation of non-coding RNAs. *Nature.* 2008; 456(7218):130–4. Epub 2008/09/30. doi: nature07348 [pii] <https://doi.org/10.1038/nature07348> PMID: 18820678.
  30. Hirota K, Mizuno K, Shibata T, Ohta K. Distinct chromatin modulators regulate the formation of accessible and repressive chromatin at the fission yeast recombination hotspot ade6-M26. *Mol Biol Cell.* 2008; 19(3):1162–73. Epub 2008/01/18. doi: E07-04-0377 [pii] <https://doi.org/10.1091/mbc.E07-04-0377> PMID: 18199689; PubMed Central PMCID: PMC2262960.
  31. Braafladt S, Reipa V, Atha DH. The Comet Assay: Automated Imaging Methods for Improved Analysis and Reproducibility. *Sci Rep.* 2016; 6:32162. <https://doi.org/10.1038/srep32162> PMID: 27581626; PubMed Central PMCID: PMC5007470.
  32. Breslin C, Clements PM, El-Khamisy SF, Petermann E, Iles N, Caldecott KW. Measurement of chromosomal DNA single-strand breaks and replication fork progression rates. *Methods Enzymol.* 2006; 409:410–25. Epub 2006/06/24. doi: S0076-6879(05)09024-5 [pii] [https://doi.org/10.1016/S0076-6879\(05\)09024-5](https://doi.org/10.1016/S0076-6879(05)09024-5) PMID: 16793415.
  33. Kohn KW. Principles and practice of DNA filter elution. *Pharmacol Ther.* 1991; 49(1–2):55–77. Epub 1991/01/01. doi: 0163-7258(91)90022-E [pii]. PMID: 1852788.
  34. Kohn KW. DNA filter elution: a window on DNA damage in mammalian cells. *Bioessays.* 1996; 18(6):505–13. Epub 1996/06/01. <https://doi.org/10.1002/bies.950180613> PMID: 8787538.
  35. Bradley MO, Kohn KW. X-ray induced DNA double strand break production and repair in mammalian cells as measured by neutral filter elution. *Nucleic Acids Res.* 1979;(3):793–804. Epub 1979/10/10. PMID: 92010; PubMed Central PMCID: PMC328056.
  36. Fisher AE, Hohegger H, Takeda S, Caldecott KW. Poly(ADP-ribose) polymerase 1 accelerates single-strand break repair in concert with poly(ADP-ribose) glycohydrolase. *Mol Cell Biol.* 2007; 27(15):5597–



605. Epub 2007/06/06. doi: MCB.02248-06 [pii] <https://doi.org/10.1128/MCB.02248-06> PMID: 17548475; PubMed Central PMCID: PMC1952076.
37. Gottschalk AJ, Timinszky G, Kong SE, Jin J, Cai Y, Swanson SK, et al. Poly(ADP-ribose)ylation directs recruitment and activation of an ATP-dependent chromatin remodeler. *Proc Natl Acad Sci U S A*. 2009; 106(33):13770–4. Epub 2009/08/12. doi: 0906920106 [pii] <https://doi.org/10.1073/pnas.0906920106> PMID: 19666485; PubMed Central PMCID: PMC2722505.
  38. Murai J, Huang SY, Das BB, Renaud A, Zhang Y, Doroshov JH, et al. Trapping of PARP1 and PARP2 by Clinical PARP Inhibitors. *Cancer Res*. 2012; 72(21):5588–99. <https://doi.org/10.1158/0008-5472.CAN-12-2753> PMID: 23118055; PubMed Central PMCID: PMC3528345.
  39. Dantzer F, Menissier-de Murcia J, Barlow C, Wynshaw-Boris A, de Murcia G. Poly(ADP-ribose) polymerase activity is not affected in ataxia telangiectasia cells and knockout mice. *Carcinogenesis*. 1999; 20(1):177–80. Epub 1999/02/06. PMID: 9934867.
  40. Yoshimura M, Kohzaki M, Nakamura J, Asagoshi K, Sonoda E, Hou E, et al. Vertebrate POLQ and POLbeta cooperate in base excision repair of oxidative DNA damage. *Mol Cell*. 2006; 24(1):115–25. Epub 2006/10/05. doi: S1097-2765(06)00534-X [pii] <https://doi.org/10.1016/j.molcel.2006.07.032> PMID: 17018297; PubMed Central PMCID: PMC1868411.
  41. Hong Z, Jiang J, Hashiguchi K, Hoshi M, Lan L, Yasui A. Recruitment of mismatch repair proteins to the site of DNA damage in human cells. *J Cell Sci*. 2008; 121(Pt 19):3146–54. <https://doi.org/10.1242/jcs.026393> PMID: 18765568.
  42. Lan L, Nakajima S, Oohata Y, Takao M, Okano S, Masutani M, et al. In situ analysis of repair processes for oxidative DNA damage in mammalian cells. *Proc Natl Acad Sci U S A*. 2004; 101(38):13738–43. <https://doi.org/10.1073/pnas.0406048101> PMID: 15365186; PubMed Central PMCID: PMC1868411.
  43. Okano S, Kanno S, Nakajima S, Yasui A. Cellular responses and repair of single-strand breaks introduced by UV damage endonuclease in mammalian cells. *J Biol Chem*. 2000; 275(42):32635–41. Epub 2000/08/05. <https://doi.org/10.1074/jbc.M004085200> [pii]. PMID: 10924509.
  44. Barretina J, Caponigro G, Stransky N, Venkatesan K, Margolin AA, Kim S, et al. The Cancer Cell Line Encyclopedia enables predictive modelling of anticancer drug sensitivity. *Nature*. 2012; 483(7391):603–7. <https://doi.org/10.1038/nature11003> PMID: 22460905; PubMed Central PMCID: PMC3320027.
  45. Gottschalk AJ, Trivedi RD, Conaway JW, Conaway RC. Activation of the SNF2 family ATPase ALC1 by poly(ADP-ribose) in a stable ALC1.PARP1.nucleosome intermediate. *J Biol Chem*. 2012; 287(52):43527–32. <https://doi.org/10.1074/jbc.M112.401141> PMID: 23132853; PubMed Central PMCID: PMC3527939.
  46. Sellou H, Lebeaupin T, Chapuis C, Smith R, Hegele A, Singh HR, et al. The poly(ADP-ribose)-dependent chromatin remodeler Alc1 induces local chromatin relaxation upon DNA damage. *Mol Biol Cell*. 2016; 27(24):3791–9. <https://doi.org/10.1091/mbc.E16-05-0269> PMID: 27733626; PubMed Central PMCID: PMC5170603.